FERROMAGNETIC RESONANCE OF FeNi/Cu/FeNi THIN FILM ON COPLANAR WAVEGUIDE WITH OPERATING FREQUENCY OF 1 TO 20 GHz

S. V. Shcherbinin,[1,2] **S. O. Volchkov,**[1,3] **Ch. Swindells,**[3] **B. Nicholson,**[3] **D. Atkinson,**[3] **and G. V. Kurlyandskaya** [1,4]

The paper presents the calculation results of the coplanar waveguide geometry using the method of conformal mapping and computerized simulation with COMSOL Multiphysics software. Ferromagnetic FeNi/Cu/FeNi magneto-sensitive elements are fabricated in one cycle with the coplanar waveguide which conveys drive signals. Magnetodynamics of the obtained film structures is studied within the frequency range of 1–20 GHz. It is shown that the main parameters of ferromagnetic resonance can be found for the thin film structures on the coplanar waveguide.

Keywords: electromagnetic absorption, magnetic films, coplanar waveguide, ferromagnetic resonance, magneto-sensitive elements.

INTRODUCTION

Ferromagnetic materials are widely used in ultra-high frequency (UHF) devices which include switches, circulators, controllable phase shifters, inductors, external magnetic field detectors, *etc*. [1–4]. Although ferrites are mostly used in microwave applications (due to no eddy current losses) [5], recent decades have seen an increased interest in developing microwave devices based on magnetic thin films [6, 7]. Owing to the development of techniques for depositing metallic and nanostructured films onto dielectric substrates [8], ferromagnetic devices with functional elements of a microscopic size are now available to researchers and engineers [8, 9].

In UHF techniques, it is impossible to produce integrated circuits or printed circuit boards with not allowing for the parameters of microstrips, coplanar waveguides and other transmission lines [10]. Integrated circuits operating in the super high frequency (SHF) band are mainly based on microstrips, as the transmission lines and lines discontinuities of several micrometers are thousands times less than the electromagnetic radiation wavelength. In the production of printed circuit boards, coplanar waveguides are used wherever possible.

In microwave devices, microstrips and coplanar waveguides find use for matching ferromagnetic thin films [1] as depicted in Fig. 1. In analyzing the parameters of ferromagnetic resonance (FMR) [11, 12] and magnetic impedance [2, 3] of thin films, the operating range of the ferromagnetic film on a microstrip significantly reduces to about 3 GHz [13]. This is because the mismatch between the wave impedance of the microstrip line and the coplanar waveguide with a ferromagnetic film and also radiation losses with increasing operating frequency.
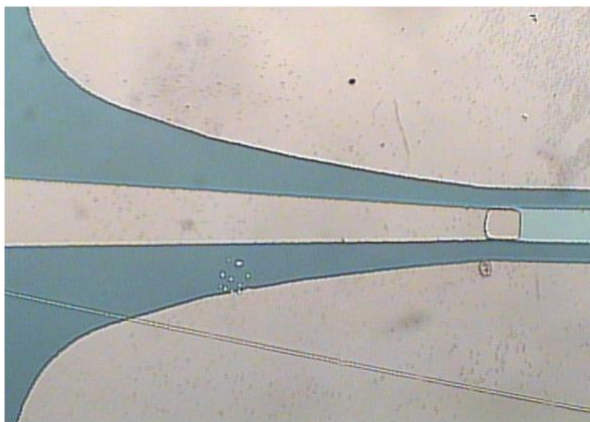

Fig. 1. Optical image of the contact connection between the coplanar waveguide and sandwiched FeNi/Cu/FeNi film.

A fabrication of magneto-sensitive elements in one cycle with coplanar waveguides is more preferable both for research and integrated microelectronics highly demanding miniaturization of components. FeNi-based film macro- and nanostructures are used in hardware components of spintronics and magnetic sensors [13, 14]. The quasi-two-dimensional magnetodynamic nature of these structures does not provide a constant demagnetizing field along the long film side. Due to strong shape anisotropy, this configuration is stable even with nonzero remanence [15].

In this work, we calculate the coplanar waveguide geometry using the method of conformal mapping and computerized simulation. $Fe_{19}Ni_{81}/Cu/Fe_{19}Ni_{81}$ magneto-sensitive elements are fabricated in one cycle with the coplanar waveguide which conveys drive signals. It is shown that the main parameters of ferromagnetic resonance of the thin film structure, which is a center strip conductor on the coplanar waveguide, can be measured within the frequency range of 1–20 GHz.

MATERIALS AND METHODS

In accordance with the aim of this work to calculate the main FMR parameters of the FeNi film in a 1–20 GHz frequency range, let us find a design solution for the coplanar waveguide transmission line. Its configuration, whose schematic representation is given in Fig. 2, allows embedding a ferromagnetic strip, the wave impedance remaining constant along the whole transmission line owing to varying the gap g. Moreover, the radiation of the matched coplanar waveguide in the environment is insignificant due to the electromagnetic field concentrated nearby the conducting surfaces. The ferromagnetic film sensitivity to the external magnetic field is proportional to the length-to-width ratio. It is therefore expedient to consider the width w and the length l of the ferromagnetic film. The wave impedance matching is provided by the appropriate gap width. The thickness of the dielectric and conducting layers h and t should also be taken into consideration.
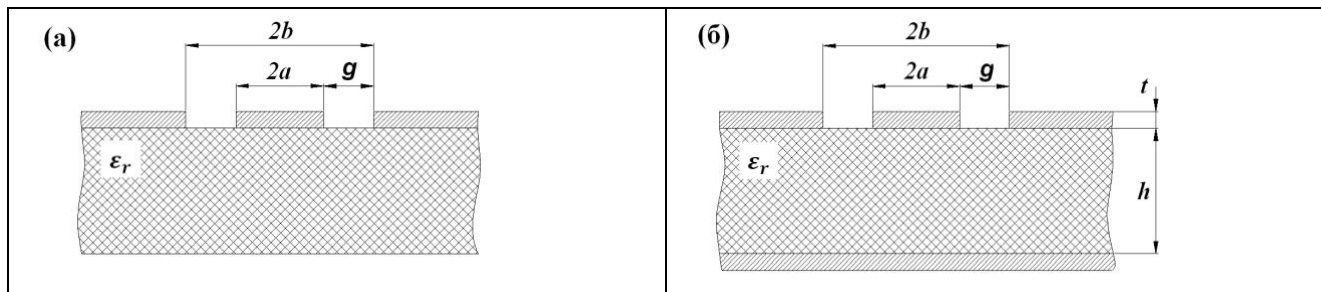

Fig. 2. Cross-sectional view of coplanar waveguide transmission line: a – ungrounded, b – grounded.

The geometrical parameters of the coplanar waveguide with the center strip conductor are calculated using the equations obtained by the method of conformal mapping and computerized simulation.

Coplanar waveguide geometry calculated by equations using the method of conformal mapping

When measuring the width ($w = 2a$) of the center strip conductor, the method of conformal mapping keeps the real value of the wave impedance constant (50 Ohm) due to correct varying the gap width, i.e. $g = (2b – 2a)/2 = b–a$. At the same time, the thickness h of the silicon substrate remains constant, the relative permittivity ε_r is 11.7.

The wave impedance of the ungrounded coplanar waveguide is [10]:

$$Z_C = \frac{30\pi}{\sqrt{\varepsilon_{\text{eff}}}} \frac{K(k')}{K(k)} = 50 \ \Omega,$$

where

$$\varepsilon_{\text{eff}} = 1 + \frac{\varepsilon_r - 1}{2} \frac{K(k')}{K(k)} \frac{K(k_1)}{K(k_1')}$$

is the effective permittivity;

$$K(k) = \int_0^{\pi/2} \frac{d\varphi}{\sqrt{1 - k^2 (\sin \varphi)^2}}$$

is the complete elliptic integral of the first type;

$$k = \frac{a}{b}, \qquad k_1 = \frac{\sinh \dfrac{\pi a}{2h}}{\sinh \dfrac{\pi b}{2h}},$$

$$k' = \sqrt{1 - k^2}, \qquad k_1' = \sqrt{1 - k_1^2}$$

is the geometry of the ungrounded coplanar waveguide.

The wave impedance of the grounded coplanar waveguide can be found from

$$Z_C = \frac{60\pi}{\sqrt{\varepsilon_{\text{eff}}}} \frac{1}{\dfrac{K(k)}{K(k')} + \dfrac{K(k_1)}{K(k_1')}} = 50 \, [\Omega],$$

where

$$\varepsilon_{\text{eff}} = \frac{1 + \varepsilon_r \dfrac{K(k')}{K(k)} \dfrac{K(k_1)}{K(k_1')}}{1 + \dfrac{K(k')}{K(k)} \dfrac{K(k_1)}{K(k_1')}}$$

is the effective permittivity, $K(k)$ is the complete elliptic integral of the first type;

$$k = \frac{a}{b}, \qquad k_1 = \frac{\tanh \dfrac{\pi a}{2h}}{\tanh \dfrac{\pi b}{2h}},$$

$$k' = \sqrt{1 - k^2}, \qquad k_1' = \sqrt{1 - k_1^2}$$

is the geometry of the grounded coplanar waveguide.

Coplanar waveguide geometry calculated *via* computerized simulation

The geometry of the coplanar waveguide can be calculated in various simulation programs such as MWO, CST, HFSS and on-line calculators [16, 17].

We used COMSOL Multiphysics software to construct the coplanar waveguide model with the parameters of the material of the center strip conductor. This model also allowed us to introduce such physical parameters as temperature, elastic force, and others. The engineering workstation included an 32 core of Intel Xeon E5 CPU and RAM 128 Gb with parallel computing architecture. The Klopfenstein tapered line was used to minimize the electromagnetic reflection and absorption along the coplanar waveguide [18]. The permittivity in the SHF band was assumed to be equal to unity, while the specific resistance of the FeNi/Cu/FeNi film was accepted to be higher than that of copper.

FeNi/Cu/FeNi magneto-sensitive elements and the coplanar waveguide were produced both in one cycle, using a Mantis QPrep500 ultra-high vacuum (UHV) sputter deposition system (Mantis Deposition Ltd, United Kingdom) and a photolithography unit EVG 620 (EV Group, Austria). The $Fe_{19}Ni_{81}$(100 nm)/Cu(100 nm)/$Fe_{19}Ni_{81}$(100 nm) structure represented the rectangular films 1000 μm long and 25–100 μm wide. The wave impedance matching was provided by the appropriate gap width (see Fig. 2). Thermally oxidized single crystal silicon plates were used as substrates.

Frequency dependencies of the elements of a scattering matrix or FMR parameters were measured at 0.1–20 GHz and –10 dBm on a ZVA67 Network Analyzer (Rohde & Schwarz, Germany) using the dual-port method [19]. For measurements, the element holder was placed between the electromagnet poles. A constant external field was applied along the wave vector in the UHF path.

RESULTS AND DISCUSSION

According to the obtained parameters, 42 coplanar waveguides with the center strip conductor on the FeNi/Cu/FeNi film structure were fabricated on 7.5×9.0 mm silicon substrates. The center strip conductor was 1.0 mm long and 25 to 100 μm wide. The Klopfenstein tapered line was used to match the center strip conductor with the ports (see Fig. 1). The coplanar waveguides were manufactured both with and without a ground plane.

The geometrical parameters of the coplanar waveguides were calculated by different methods differ insignificantly. According to the diagrams shown in Figs 3 and 4, the use of the ungrounded coplanar waveguide is more preferable than the grounded. This is because a) the parameter spread has less effect on the wave impedance and b) a loss of the coplanar waveguide advantages over a microstrip line due to a sharp increase in the gap, when the width of the center strip conductor is over 30 μm.
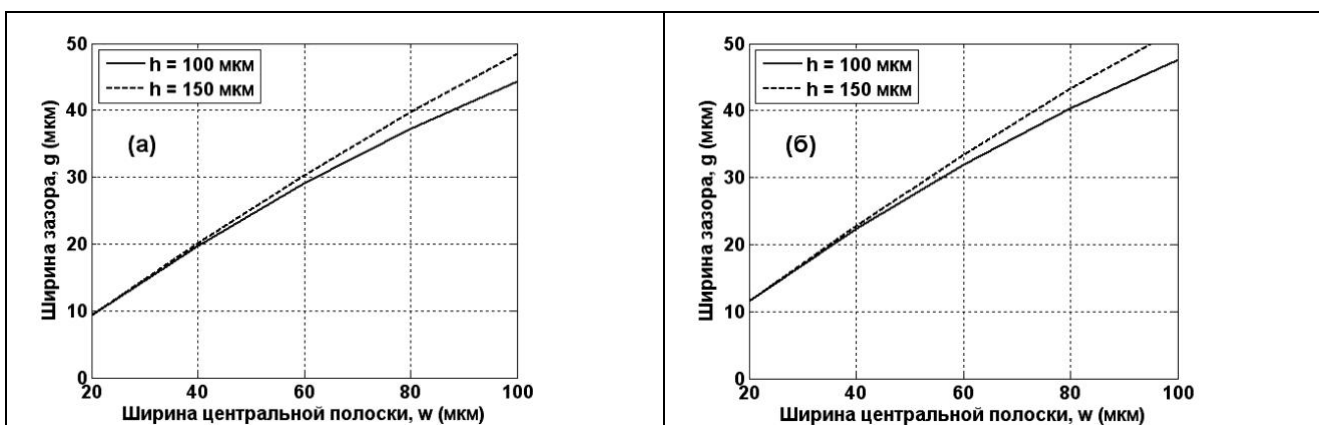

Fig. 3. Dependencies between the width of the gap and the center strip conductor of the ungrounded coplanar waveguide: *a* – conformal mapping, *b* – computerized simulation.
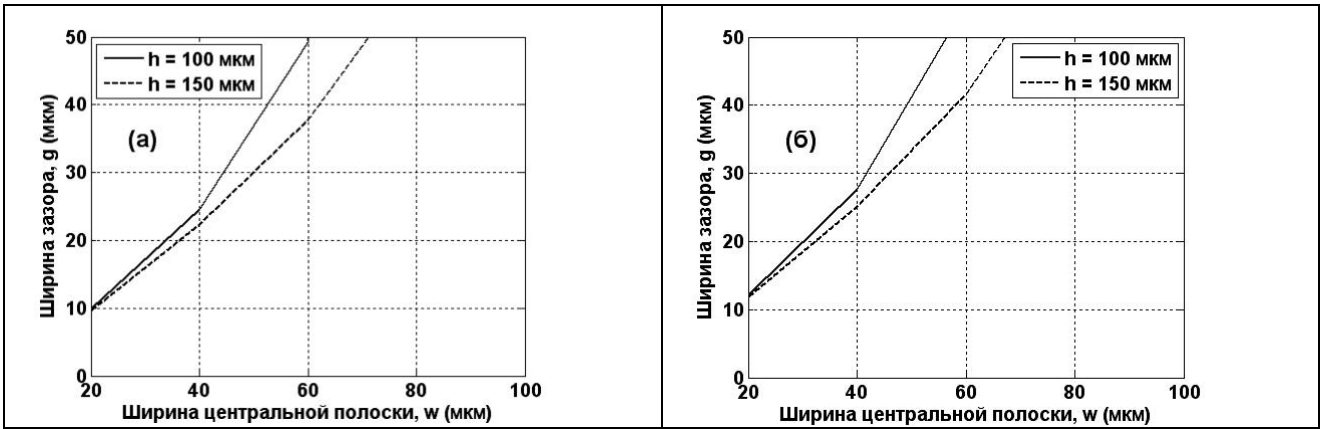
Fig. 4. Dependencies between the width of the gap and the center strip conductor of the grounded coplanar waveguide: *a* – conformal mapping, *b* – computerized simulation.

For measurements of the FMR parameters, the FeNi/Cu/FeNi films were adhered to the holder with RS conductive adhesive (RS Components, United Kingdom). The holder is made of FR-4 epoxy laminate material and operates at 20 GHz critical frequency. The photograph of this coplanar waveguide is presented in Fig. 5. The holder is equipped with SMA connectors to the network analyzer and can be then placed into a cylindrical aluminum shield. Key specifications for this measuring system are given in Table 1.
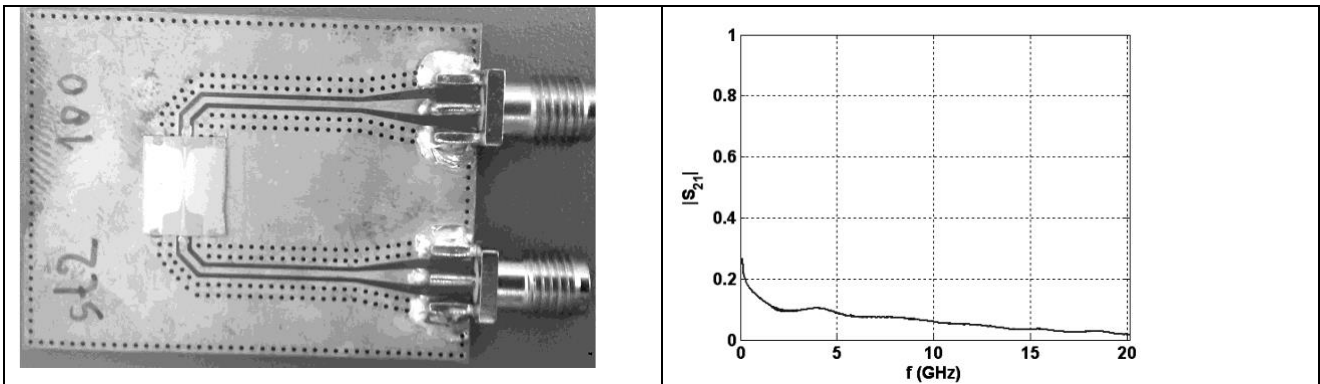

Fig. 5. Photograph of the coplanar waveguide on the holder (*a*). Frequency dependence of the absolute value of the transmission parameter S_{21} of the coplanar waveguide with FeNi/Cu/FeNi film strcuture (*b*).

TABLE 1. Key Parameters for the UHF Measuring System

Parameters to be measured	S_{11}, S_{12}, S_{21}, S_{22}
Wave impedance	50 Ohm
Frequency range	1–20 GHz
High output power	–10 dBm = 0.1 mW
Magnetic intensity range	–4 ÷ 4 kOe
Number of measurements for averaging	5
Measurement accuracy	< 1%

Microwave spectroscopy showed that most of the coplanar waveguides retain the properties of the terminated transmission line on frequencies down to 6 GHz, *i.e.* much lower than the expected limit. With increasing frequency, undesirable phenomena were suddenly observed in the ungrounded coplanar waveguide. Only a few grounded coplanar waveguides with the center strip conductor of minimum width (25 μm) were suitable for operation up to the critical frequency of 14 GHz. One such coplanar waveguide did not distort the signal up to 20 GHz, which was critical to this

measuring system (Fig. 5*b*). The FeNi/Cu/FeNi film structure on a coplanar waveguide in integrated circuits can be probably used at higher frequencies also.

The explanation of the advantage of the grounded coplanar waveguide over the ungrounded is simple. In the latter, as shown in Fig. 6*a*, the influence of foreign metallic objects such as an aluminum shield or magnet is much higher; the influence of h_2 distance to the shield becomes critical as well as the state of the non-metallic dielectric surface.
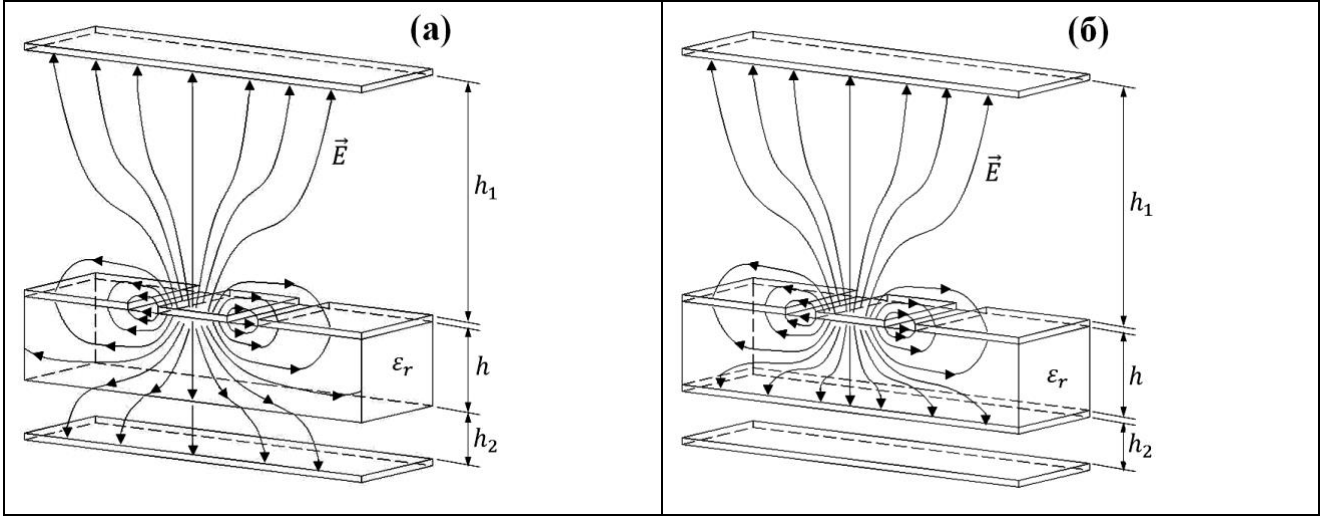

Fig. 6. Schematic of the shield effect on the ungrounded (*a*) and grounded (*b*) coplanar waveguides. Electric-field lines during electromagnetic wave propagation along the coplanar waveguide.

The shield effect should be considered, because the coplanar waveguide circuits will always be in proximity to a shield [20]. The ground layer in the coplanar waveguide considerably weakens the influence of external objects, especially at decreasing width of the center strip conductor and gaps (Fig. 6*b*). A 100 μm thick silicon substrate requires 25 μm wide strips and, consequently, narrow gaps. It is rather difficult to ensure the necessary accuracy of such a configuration at the current level of technology.

Many coplanar waveguide samples demonstrate the electromagnetic absorption in the constant external field. But the coplanar waveguide mismatch does not allow us to study the FMR parameters in the entire frequency range. Figure 7 *a* shows the frequency dependence of the relative loss $\Delta P/P$ of the electromagnetic radiation at 1–20 GHz for the grounded coplanar waveguide with the center strip conductor 25 μm wide. The dependence between the resonant absorption of the thin film and the external field is derived from the Kittel formula [11]:

$$\left(\frac{\omega}{\gamma}\right)^2 = (H_{\text{res}} + H_K)(H_{\text{res}} + H_K + 4\pi M_S),\qquad(1)$$

where $\omega = 2\pi f$ is the cyclic frequency of microwave radiation, γ is the gyromagnetic ratio, H_{res} is the resonance field, H_K is the anisotropy field, M_S is the saturation magnetization. The theoretical dependence in Fig. 7*b* is derived from Eq. (1) at $H_K = 8$ Oe, $M_S = 810$ G [2, 14].
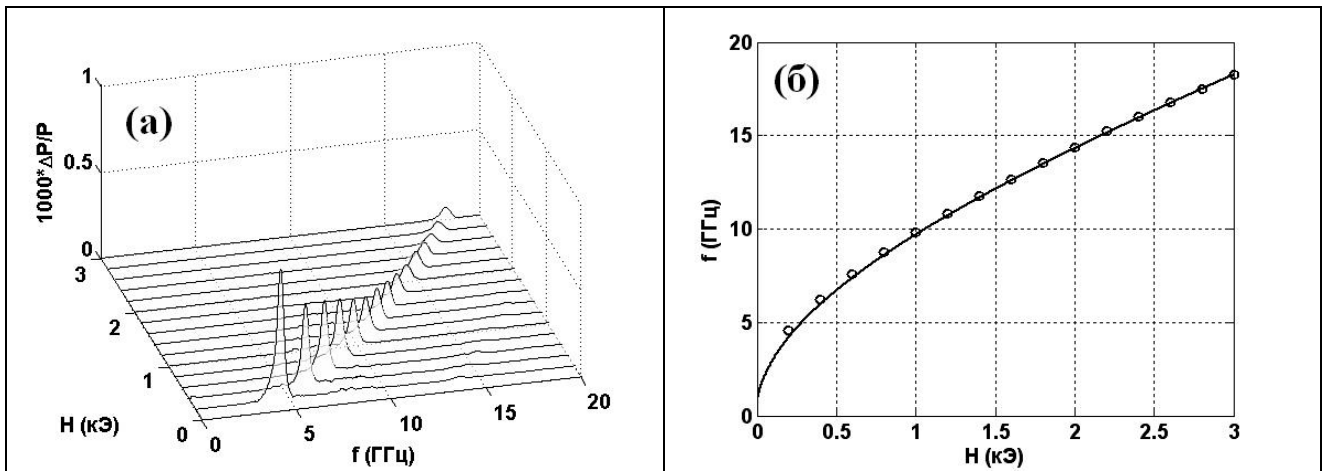
Fig. 7. Frequency dependence of the relative loss of the electromagnetic radiation for the grounded coplanar waveguide with the FeNi/Cu/FeNi film (*a*). Dependence between the resonant absorption and the external field: experimental (circles) and theoretical (solid line) results derived from the Kittel formula (*b*).

Good agreement of experimental data and theoretical calculations demonstrates the ferromagnetic resonance observed for the ferromagnetic thin film. This technique can therefore be applied in studying the FMR parameters and developing miniature devices utilizing this phenomenon in the microwave band. Moreover, rather high values of S_{21} parameter ranging within 0–4 kOe and 1–20 GHz of the external field make it possible to apply this measuring system in different technologies.

CONCLUSIONS

The coplanar waveguide geometry was calculated by using the method of conformal mapping and computerized simulation with COMSOL Multiphysics software. Ferromagnetic $Fe_{19}Ni_{81}/Cu/Fe_{19}Ni_{81}$ magneto-sensitive elements were fabricated in one cycle with the coplanar waveguides demanded in various technological applications. It was shown that the main FMR parameters could be found for the thin film structures within the frequency range of 1–20 GHz.

REFERENCES

1. L. F. Chen, C. K. Ong, C. P. Neo, *et al.,* Microwave Electronics: Measurement and Materials Characterization, John Wiley & Sons, Ltd., New York (2004).
2. S. O. Volchkov, A. V. Svalov, and G. V. Kurlyandskaya, Russ. Phys. J., **52**, No. 8, 769–776 (2009).
3. A. Antonov, S. Gadetsky, A. Granovsky, *et al.,* Physica A, **241**, 414–419 (1997).
4. D. S. Gardner, G. Schrom, F. Paillet, *et al.,* IEEE Trans. Magn., **45**, No. 10, 4760–4766 (2009).
5. Y. F. Chen, K. T. Wu, Y. D. Yao, *et al.,* Microelectron. Eng., **81**, 329–335 (2005).
6. A. B. Rinkevich, Ya. A. Pakhomov, E. A. Kuznetsov, *et al.,* Tech. Phys. Lett., **45**, No. 3, 225–227 (2019).
7. M. A. Corrêa, F. Bohn, A. D.C. Viegas, *et al.,* JMMM, **320**, No. 14, e25–e28 (2008).
8. A. García-Arribas, E. Fernandez, A. Svalov, *et al.,* JMMM, **400**, 321–326 (2016).

9. G. Buettel, J. Joppich, and U. Hartmann, Appl. Phys. Lett., **111**, 232401 (2017).
10. C. Nguyen, Analysis Methods for RF, Microwave, and Millimeter-Wave Planar Transmission Line Structures, John Wiley & Sons, Inc., New York (2003).
11. C. Kittel, Introduction to Solid State Physics, USA, Wiley, New York (1996).
12. S. M. Bhagat, from Metals Handbook, vol. 10, ASM International, Metals Park, Ohio (1986).
13. J. M. Gonzalez, A. Garcia-Arribas, S. V. Shcherbinin, *et al.,* Measurement, **126**, 215–222 (2018).
14. N. A. Buznikov, A. P. Safronov, I. Orue, *et al.,* Biosens. Bioelectron., **117**, 366 (2018).
15. J. Ding, M. Kostylev, and A. O. Adeyeye, Phys. Rev. B, **84**, 054425 (2011).
16. Yu. E. Mitel'man, Automated Design of Microwave Devices in AWRDE [in Russian], UrFU, (2012).
17. S. E. Bankov, A. A. Kurushin, and V. D. Razevig, Analysis and Optimization of Microwave Devices Using HFSS [in Russian], Solon-Press, Moscow (2004).
18. X. Yao and N. A. F. Jaeger, in: Proc. Conf. "Photonics North", **8007**, 80070G (2011).
19. S. V. Shcherbinin, S. O. Volchkov, V. N. Lepalovskii, *et al.,* Russ. J. Nondestruct., **53**, No. 3, 204-212 (2017).
20. R. N. Simons, Coplanar Waveguide Circuits, Components, and Systems, John Wiley & Sons, Inc., New York (2001).